Vol. 29 (1998) *ACTA PHYSICA POLONICA B* No 12

CHIRAL RANDOM MATRIX MODELS IN QCD*

Romuald A. Janik

Service de Physique Théorique, CEA Saclay, 91191, Gif-sur-Yvette, France
Department of Physics, Jagellonian University
Reymonta 4, 30-059, Kraków, Poland

Maciej A. Nowak

Department of Physics, Jagellonian University
Reymonta 4, 30-059, Kraków, Poland
GSI, Planckstr. 1, D-64291 Darmstadt, Germany

Gábor Papp

CNR Department of Physics, KSU, Kent, Ohio 44242, USA
Institute for Theoretical Physics, Eötvös University, Budapest, Hungary

and Ismail Zahed

Department of Physics and Astronomy, SUNY
Stony Brook, New York 11794, USA

(Received December 12, 1998)

We review some motivation behind the introduction of chiral random matrix models in QCD, with particular emphasis on the importance of the Gell-Mann–Oakes–Renner (GOR) relation for these arguments. We show why the microscopic limit is universal in power counting, and present arguments for why the macroscopic limit is generic for a class of problems that defy power counting, examples being the strong CP and U(1) problems. We also discuss some of our new results in light of recent lattice simulations.

PACS numbers: 12.38.Lg

* Presented at the XXXVIII Cracow School of Theoretical Physics, Zakopane, Poland, June 1–10, 1998.

1. Introduction

It is well known that the spontaneous breaking of chiral symmetry in QCD along with its explicit breaking, provide stringent constraints on on-shell amplitudes [1], whether at threshold or beyond. These constraints can be exploited in power counting (ChPT) [2], or to any order [3], leading to a comprehensive description of a number of reaction processes. The same symmetry constrains the off-shell amplitudes such as the vacuum to vacuum amplitude in the presence of external sources.

What is less well-known perhaps, is the fact that in a finite Euclidean volume $V = L^4$ similar constraints are still in action even in the case where the box size L is smaller than the pion Compton wavelength $1/\sqrt{m}$ (in units where the QCD scale $\Lambda = 1$). This is a regime where the spontaneous breaking of chiral symmetry is obsolete. This observation for the off-shell amplitudes was first emphasized by Gasser and Leutwyler [4]. Their observation carries to most models with spontaneously broken symmetries in $d > 2$ as was discussed by Hasenfratz and Leutwyler [5].

The regime for which $mV > 1$ will be referred to as macroscopic. In it, chiral symmetry is spontaneously broken with $\langle q^\dagger q\rangle = 1$ (again in units where $\Lambda = 1$). The regime for which $mV < 1$ will be referred to as microscopic. In it, chiral symmetry is effectively restored with $\langle q^\dagger q\rangle = mV + \mathcal{O}$. The nature of the corrections $\mathcal{O}$ will be discussed below. The regime $mV \sim 1$ will be referred as transitional. In it, chiral symmetry is about to be restored or broken depending on how we wish to look at it. Throughout, the box size is chosen $L > 1/\Lambda = 1$, so that nonperturbative effects are present. At small but finite temperature, a similar classification holds in Euclidean space with $V = \beta L^3$.

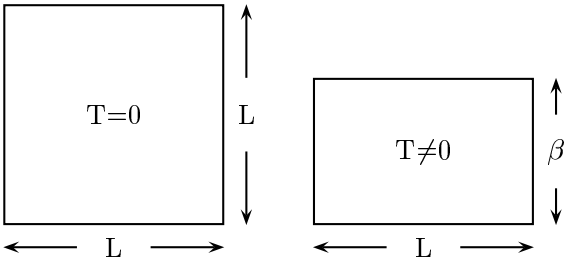

Fig. 1. QCD in a symmetric (left) and asymmetric (right) box.

The importance of the parameter mV for the constant mode problem in QCD was first noted by Jolicoeur and Morel [6] in the strong coupling regime. This remark is important as it implies that the observations to follow carry for both strong and weak coupling provided that a continuous symmetry is broken spontaneously with the occurrence of Goldstone bosons.

In the present work, we will go over a number of observations in the context of chiral symmetry that paves the road for the onset of chiral random matrix models in QCD with their relevance to the three regimes of mV detailed above. In Section 2, we go over the original observation by Banks and Casher [7]. In Section 3, we detail some of the arguments given by Gasser and Leutwyler [4] regarding the finite volume partition function, paying particular attention to the Gell-Mann–Oakes–Renner (GOR) relation. In Section 4, we summarize how these observations were used by Leutwyler and Smilga [8] to derive spectral sum rules, and derive new spectral sum rules for generalized GOR relation. In Section 5, we present simple arguments for why these sum rules are minimally reproduced by chiral random matrix models. In Section 6, we go over the construction by Verbaarschot and Zahed [9] for the microscopic n-point correlation functions as the master formulas for all diagonal and off-diagonal sum rules. The n-point correlation functions specify the degree of flavor mixing in the n-vacua, and uniquely condition the bulk spectral rigidity and level variance. The relevance of these observations for lattice simulations in symmetric and asymmetric boxes is discussed. In Section 7, we discuss the microscopic spectral density in the double scaling limit, following the original arguments by Jurkiewicz, Nowak and Zahed [10] and more recently Damgaard and Nishigaki [11] and Wilke, Guhr and Wettig [12]. New sum rules with decoupled sea and valence quark effects are discussed. We argue that the associated spectral density in the double scaling limit is universal in QCD, within a range of quark masses that we discuss. In Section 8, we put forward arguments for why chiral random matrix models are of interest in the macroscopic regime, especially when chiral power counting breaks down. We illustrate our points for the CP and U(1) problems. In Section 9 we summarize our conclusions.

2. Quark spectrum

In the early 80's Banks and Casher made a remarkable observation regarding the relation of the quark condensate to the QCD quark spectrum. In an Euclidean volume V, they noticed that the amount of quark pair condensation $\langle q^\dagger q\rangle$ relates in a simple way to the distribution of quark eigenvalues $\nu(\lambda)$. Indeed,

$$\begin{aligned} V\langle q^\dagger q\rangle &= \sum_k \langle \frac{1}{\lambda_k + im}\rangle \\ &= \int d\lambda \frac{1}{\lambda + im}\langle \mathrm{Tr}\delta(\lambda - iD)\rangle \\ &= \int d\lambda \frac{-im}{\lambda^2 + m^2}\nu(\lambda) \to -i\pi\,\nu(m)\,, \end{aligned} \tag{1}$$

where the limit is understood for $mV > 1$. The quark eigenvalues λ_k depends implicitly on the given gauge configuration, through the eigenvalue equation $iD\,q_k = \lambda_k\,q_k$. They are paired, since $[\gamma_5, iD]_+ = 0$. This pairing causes $\nu(\lambda)$ to be an even function on its support. The averaging in (1) is over the gauge configurations.

In (1) the zero virtuality point $\lambda = 0$ [1] is the analogue of a Fermi surface. This observation suggests in fact that the regime $mV > 1$, in which chiral symmetry is spontaneously broken, is actually diffusive [14], following the delocalization of the quark eigenmodes.

More remarkably, however, is the fact that for the pair condensate to be non-zero, the density of quark eigenmodes near zero virtuality has to *grow* with the volume V. In other words, the level spacing of the quark eigenmodes in a finite volume V and near zero has to scale as $1/V$ in sharp contrast to the level spacing of a free particle in the same box which has to scale as $1/L$.

The spontaneous breaking of chiral symmetry causes a large accumulation of quark eigenmodes near zero virtuality as pictured in Fig. 2, for a fixed gauge-configuration. The occurrence of exact zero modes of the nonzero n (winding number) configuration is geometrical and follows from the topological character of the background gauge configuration. Conversely, any model that breaks spontaneously the underlying chiral symmetry displays a spectrum of the type shown in Fig. 2. This means QCD, instanton models, NJL models, *etc.*

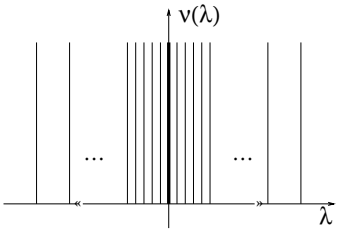

Fig. 2. Quark spectrum in the vacuum.

3. Finite volume partition function

3.1. With GOR

Few years later, Gasser and Leutwyler [4] noticed that in a finite volume V for which the Compton wavelength of the pion is large, that is $mV < 1$ but

[1] The quark virtuality λ is analogous to a complex mass in 4d Euclidean space, or an energy in 1+4d Minkowski space.

$L > 1$, while chiral symmetry is effectively restored with $\langle q^\dagger q\rangle = mV + \mathcal{O}$, the way it is restored is still uniquely conditioned by the way chiral symmetry is about to be spontaneously broken. For QCD this observation is natural if we were to approach the microscopic regime $mV < 1$ from the macroscopic regime $mV > 1$ by fine tuning the bare quark mass m.

***mV* > 1 region:** In a finite Euclidean box V the finite volume partition function Z is the sum of zero-point motions of singlet excitations: pions, kaons, nucleons, *etc.* (Casimir effect). In the regime $mV > 1$ the spontaneous breaking of chiral symmetry together with the Gell-Mann–Oakes–Renner (GOR) relation [15] allows for a book-keeping of $\ln Z$ by using chiral power counting with a typical momentum scale p, where $U \sim p^0$, $1/L \sim p$ and $m \sim m_\pi^2 \sim p^2$ and $m^2V \sim 1$ fixed. In this book-keeping, the contribution to order p^2 is given by the following Lagrangian [4]

$$\mathcal{L}_2 = \frac{F^2}{4}\mathrm{Tr}\left(\partial_\mu U^\dagger \partial_\mu U\right) - \frac{1}{2}\Sigma\ \mathrm{Tr}(mU + U^\dagger m^\dagger) \tag{2}$$

for N_f flavors with $U = e^{i\hat{\pi}/F}$ ($\hat{\pi} = \pi^\alpha \lambda_\alpha$) an SU($N_\mathrm{f}$) valued field subject to the boundary condition $U(x + L) = U(x)$. The normalization is chosen $\mathrm{Tr}\lambda_\alpha\lambda_\beta = 2\delta_{\alpha,\beta}$. Throughout we will use m for either the non-degenerate case $m = (m_1, ..., m_{N_\mathrm{f}})$ or the degenerate case $m = m\mathbf{1}_{N_\mathrm{f}}$. We hope that the reference to each case will be clear from the notation used.

In a periodic box, the free pion propagator is

$$G_\pi(x) = \frac{1}{V}\sum_{k_n} \frac{\mathrm{e}^{-ik_n x}}{k_n^2 + m_\pi^2} = \frac{1}{Vm_\pi^2} + \frac{1}{V}{\sum_{k_n}}' \frac{\mathrm{e}^{-ik_n x}}{k_n^2 + m_\pi^2}\,, \tag{3}$$

where the primed sum is over non-zero four momenta with $k_n = (n_1, n_2, n_3, n_4)2\pi/L$. To order p^2 the pion mass is $m_\pi^2 = m\Sigma/F^2 \sim m$ and the condensate is $-\langle\bar{q}q\rangle = \Sigma$. To order p^4, the one-loop contribution from (2) has to be supplemented with the most general terms consistent with broken chiral symmetry and general principles [4] (Lorentz invariance is upset in a box to order p^4).

***mV* < 1 region**: In the microscopic regime $1 > mV$, the zero mode contribution $1/mV$ in (3) dwarfs the non-zero mode contributions (primed sum) causing the chiral power counting to break down. In this regime Gasser and Leutwyler suggested a reorganization of the chiral power counting fixing mV instead of m^2V with expansion in $\varepsilon = 1/L$, thereby allowing for a systematic resummation of the pionic zero modes in the finite volume partition function.

To order $\mathcal{O}(\varepsilon^2)$ the dependence of $Z[S,P,V]$ on the external sources $S = m\Sigma/2 + S'$ and P is simply

$$Z[S,P,V] = N[0] \int\limits_{\mathrm{SU}(N_\mathrm{f})} dU \, \mathrm{e}^{V\,\mathrm{Tr}((S+iP)U+\mathrm{h.c.})} . \tag{4}$$

$N[0]$ receives contribution from the non-zero mode terms, essentially the Casimir energy of free pions in a box V as indicated by the first diagram in Fig. 3. This contribution is S,P-independent to the order quoted. For $x = m\Sigma V$ and $N_\mathrm{f} = 1$, $Z[m] \sim \mathrm{e}^x$, while for $N_\mathrm{f} = 2$ with equal masses it is $Z[m] \sim I_1(2x)/2x$ [4]. For one massive flavor and $N_\mathrm{f} - 1$ massless flavors it is $Z[m] \sim I_{N_\mathrm{f}-1}(x)/x^{N_\mathrm{f}-1}$. In each case, $Z[m] = Z[m,0,V]$ and the proportionality constant is m independent.

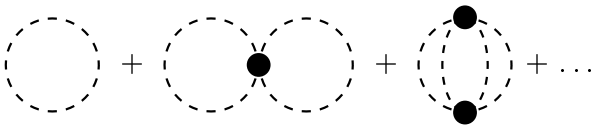

Fig. 3. Meson contribution to $\ln Z$ for $mV > 1$.

From (4) the chiral condensate to order $\mathcal{O}(\varepsilon^2)$ is

$$i\langle q^\dagger q\rangle = -\frac{N[0]}{Z[m]}\frac{\Sigma}{2} \int\limits_{\mathrm{SU}(N_\mathrm{f})} dU \, \mathrm{Tr}(U+U^\dagger)\mathrm{e}^{\frac{1}{2}m\Sigma V\,\mathrm{Tr}(U+U^\dagger)} \tag{5}$$

and vanishes as $x = mV \to 0$, to the exception of $N_\mathrm{f} = 1$ where $i\langle q^\dagger q\rangle = -\Sigma$. For $N_\mathrm{f} = 2$ and two equal masses, $i\langle q^\dagger q\rangle = -\Sigma I_2(2x)/I_1(2x)$, while for one massive and $N_\mathrm{f} - 1$ massless quarks $i\langle q^\dagger q\rangle = -\Sigma I_{N_\mathrm{f}}(x)/I_{N_\mathrm{f}-1}(x)$. In this limit all points on $\mathrm{SU}(N_\mathrm{f})$ are equally weighted. Although chiral symmetry is restored in the regime $mV < 1$, the way by which it is restored is conditioned by :

(i) the nature of the coset;

(ii) the explicit $(N_\mathrm{f}, N_\mathrm{f})$ breaking;

(iii) the underlying GOR assumption.

3.2. Without GOR

***mV* > 1 region:** The GOR assumption is important in establishing (2) as the starting point for power counting in ChPT in the macroscopic

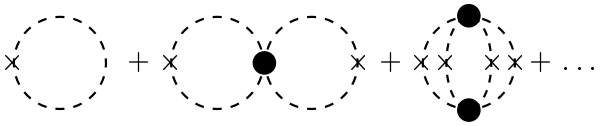

Fig. 4. Zero momentum contribution to $\ln Z$ for $mV < 1$.

regime. This assumption may be relaxed in the form of generalized ChPT. An example to order p^2 is

$$\begin{aligned}\mathcal{L}_2 = \quad & \frac{F^2}{4}\mathrm{Tr}\left(\partial_\mu U^\dagger \partial_\mu U\right) - \frac{1}{2}V\Sigma\ \mathrm{Tr}(mU + U^\dagger m^\dagger) \\ & + A\mathrm{Tr}(m^\dagger U m^\dagger U + \mathrm{h.c.}) + B\left(\mathrm{Tr}(m^\dagger U + \mathrm{h.c.})\right)^2 \\ & + C\left(\mathrm{Tr}(m^\dagger U - \mathrm{h.c.})\right)^2 + D\mathrm{Tr}(m^\dagger m) \end{aligned} \tag{6}$$

as suggested by Stern, Sazdjian and Fuchs and others [16]. Here Σ and m are counted of order p, while A, B, C, D are counted of order p^0. The constants Σ, A, B, C are low-energy parameters, while D is not (see below). To order p^2 the pion mass squared and the chiral condensate are

$$\begin{aligned} m_\pi^2 = \quad & \frac{m}{F^2}\left(\Sigma - 8mA - 8mN_\mathrm{f}B\right)\,, \\ -\langle\overline{q}q\rangle = \quad & \Sigma - m(2A + D + 4N_\mathrm{f}B)\,. \end{aligned} \tag{7}$$

The constant D is subtraction dependent. It relates to the m-dependent quadratic divergence in the condensate. It is not amenable to low-energy constraints.

***mV* < 1 region:** Since the contribution of the pionic zero modes in (3) are of the form $1/Vm_\pi{}^2$, the finite volume partition function (4) for fixed Vm_π^2 would involve A, B, C, D from (6). The microscopic limit is changed compared to the GOR assumption if we were to take Vm_π^2 fixed but small (see Section 4.2). Such a limit could be reached by varying m for fixed $m^2V < 1$. The power counting in $\varepsilon = 1/L$ would be: Σ and m of order ε^2, and A, B, C, D of order ε^0. In this regime, the chiral condensate again vanishes in the chiral limit as all points on the $\mathrm{SU}(N_\mathrm{f})$ manifold are equally weighted.

Clearly mV fixed selects the GOR form in the microscopic regime, and could be used for a precise determination of Σ by comparison to ChPT. This method may be more accurate than a simple extrapolation of the condensate to zero m, owing to finite size effects. This is more than an academic exercise since both (2) and (6) lead to the same low energy constraints, and

experiments are underway at DAPHNE to test the validity of the GOR hypothesis by firming up the accuracy of the S-wave $\pi\pi$ scattering length near threshold [17].

4. Microscopic sum rules

4.1. With GOR

In the early 90's Leutwyler and Smilga [8] remarked that the finite volume partition function could be used to derive sum rules for the quark spectrum (qualitativaly shown in Fig. 2) in the microscopic regime for gauge configurations of fixed winding number n. Assuming the concept of n-vacua for the QCD state, the finite volume partition function for fixed n relates to the finite volume partition function through

$$\begin{aligned} Z_n[m] &= \int_0^{2\pi} \frac{d\theta}{2\pi}\, \mathrm{e}^{-in\theta}\, Z[m\mathrm{e}^{i\theta/N_\mathrm{f}}] \\ &= N(0) \int_{\mathrm{U}(N_\mathrm{f})} dU\ (\det U)^n\, \mathrm{e}^{\frac{1}{2}V\Sigma\,\mathrm{Tr}(mU+U^\dagger m^\dagger)} \end{aligned} \tag{8}$$

in the microscopic regime $mV < 1$. For QCD $n = \frac{\alpha_\mathrm{s}}{8\pi}\int E^a \cdot B^a$ and is valued in $\boldsymbol{Z}$. The left-hand side in (8) involves the quark spectrum averaged over gauge configurations with fixed winding number n, while the right-hand side involves an information from the hadrons. $Z_n[m]$ is local in the quark variables, but non-local in the hadronic variables. Scalar n-point functions following from (8) do not obey the cluster decomposition.

$Z_n[m]$ does not discriminate between $N_\mathrm{f} = 1$ and $N_\mathrm{f} > 1$ in QCD. Also, $Z_n[m]$ is insensitive to the nature of the sources S' and P in (4), and only depends on the quark mass matrix chosen diagonal, and its overall phase for $n \neq 0$, since [8]

$$Z_n[\boldsymbol{V}m\boldsymbol{W}] = (\det(\boldsymbol{V}\boldsymbol{W}))^n Z_n[m]\,. \tag{9}$$

This is not the case for (4).

For one flavor, we have

$$Z_n[m] = m^{|n|} \left\langle \prod_{\lambda_k>0}{}' (\lambda_k^2 + m^2) \right\rangle_{n,A} = n!\,\mathrm{I_n}(x)\,. \tag{10}$$

with $x = mV\Sigma$ and I_n a Bessel function (the primed product does not contain the exact zero modes and the eigenvalues with negative real part).

The averaging is over the gauge configuration A with fixed winding number n. Using the infinite product representation for the Bessel function and rearranging (10) it follows that

$$\left\langle\left\langle \prod_k{}' \left(1+\frac{m^2}{\lambda_k^2}\right)\right\rangle\right\rangle_n = \prod_k \left(1+\frac{x^2}{\xi_{n,k}^2}\right), \tag{11}$$

where $\xi_{n,k}$ are the zeros of the Bessel function $J_n(\xi_{n,k})=0$ with $k=1,2,\ldots$. The double averaging on the left-hand side of (11) now includes $m^{|n|}\prod_k{}' \lambda_k^2$ as part of the measure, with a normalization to 1 at $n=0$ and $m=0$. By identifying the same powers of m on both sides of (11) sum rules for the quark eigenvalues at fixed n follow, in the microscopic regime. An example is [8]

$$\frac{1}{V^2}\left\langle\left\langle \sum_k{}' \frac{1}{\lambda_k^2}\right\rangle\right\rangle_n = \frac{\Sigma^2}{4(n+N_{\rm f})}, \tag{12}$$

where we have again reinstated Σ and $N_{\rm f}$ for convenience. The contribution of the ultraviolet modes to the primed sum in (12) vanishes like V/V^2 in the large volume limit.

It can be checked that the sum rule (12) is just a suitable arrangement of moments directly amenable to the finite volume partition function (4). They reflect therefore on the sum rules satisfied by the invariant QCD correlators at zero momentum in the microscopic limit. For example

$$\frac{1}{V^2}\left\langle\left\langle \sum_k{}' \frac{1}{\lambda_k^2}\right\rangle\right\rangle_n = \frac{\Sigma^2}{2N_{\rm f}}\int_0^{2\pi}\frac{d\theta}{2\pi}\,{\rm e}^{in\theta}\left\langle\left({\rm Tr}\left({\rm e}^{\frac{i\theta}{N_{\rm f}}}U^\dagger + U{\rm e}^{\frac{-i\theta}{N_{\rm f}}}\right)\right)^2\right\rangle_{\rm con}, \tag{13}$$

where the averaging on the rhs is done with the Haar measure normalized to 1. Notice that while the lhs is local in the quark variables, it is not on the rhs, owing to the θ integration. The rhs is the zero momentum and θ-averaged contribution from the quark susceptibility $\langle\theta|(q^\dagger q)^2|\theta\rangle$, evaluated in the microscopic limit $mV\to 0$, with $\langle q^\dagger q\rangle = 0$. The susceptibility reduces to the variance of the scalar operator on the invariant measure.

The remarkable property of (11) is that it implies that the quark spectrum near zero virtuality is indeed $1/V$ spaced, with a spacing that follows as if from a 'master' gauge field in the form $\xi_{n,k}/V$. In the microscopic regime the continuum limit $V\to\infty$ is taken by keeping the level spacing finite. The master formula for all diagonal microscopic sum rules is just given by

$$\nu_n(s=\lambda V) = \frac{1}{V}\sum_{k=1}^{\infty}\delta(\lambda-\frac{\xi_{n,k}}{V}) = \sum_{k=1}^{\infty}\delta(s-\xi_{n,k}). \tag{14}$$

The limit $V \to \infty$ with s fixed was originally discussed by Shuryak and Verbaarschot [18], and the microscopic sum rules were numerically checked to hold for the instanton liquid model. This is expected, since conditions *(i)–(iii)* at the end of Section 3.1 hold verbatim for the instanton liquid model as shown by Alkofer, Nowak, Verbaarschot and Zahed [19].

4.2. Without GOR

We note that the present results were derived starting from the GOR assumption with the ε expansion carried in the regime mV fixed but small. If the GOR relation is given up as discussed in Section 3.1, then in the regime $m_\pi^2 V \sim m^2 V$ fixed the microscopic sum rules are changed. In particular (12) becomes for $n = 0$

$$\frac{1}{V^2}\left\langle\left\langle {\sum_k}' \frac{1}{\lambda_k^2}\right\rangle\right\rangle_0 = \left[\frac{1}{4}\Sigma^2 - \frac{2}{V}(B-C)\right]\frac{\left\langle|\operatorname{Tr} U|^2\right\rangle_0}{N_{\rm f}} + \frac{D}{V}\,. \quad (15)$$

The averaging on the rhs is done over $\mathrm{U}(N_{\rm f})$ with the Haar measure. The $1/V$ term is of order ε^4, but so is Σ^2. We note, that contrary to m which is a parameter, Σ is fixed by the QCD dynamics. In small volumes V with $m_\pi^2 V$ held fixed but small, the power counting is valid, and the second term may not be negligible. The D dependence in (15) is expected from the subtraction dependence to this order.

5. Chiral random matrix models

With the renewed interest in the instanton liquid model along the lines discussed by Diakonov and Petrov [20] and also Shuryak [21], it became clear that the bulk issues elegantly revealed by the variational and statistical approach to the instanton physics are generic and likely amenable to a description in terms of random matrix theory [22]. This observation is particularly relevant for the quark eigenvalues and their correlations as originally suggested by Nowak, Verbaarschot and Zahed [23]. In this context, the relevance of the three Wigner ensembles [22] was noted earlier by Simonov [24], and the relation to the microscopic limit made by Shuryak and Verbaarschot [18]. In this limit the physics is that of a rotor for the uncolored Goldstone constant modes [2], and that of random matrix theory for the colored constant modes.

5.1. With GOR

The universality of the finite volume partition function in the microscopic regime implies that any model that satisfies the conditions *(i)–(iii)* summarized at the end of Section 3.1, will do as far as the microscopic sum rules

are concerned, thanks to the observation made by Gasser and Leutwyler [4]. The minimal model that satisfy these requirements is a four-fermi model in 0-dimension (matrix model). Specifically,

$$\mathcal{L} = q^\dagger \; im\mathrm{e}^{i\gamma_5\theta/N_\mathrm{f}} \; q + \frac{1}{V\Sigma^2} q_\mathrm{R}^\dagger q_\mathrm{L} q_\mathrm{R}^\dagger q_\mathrm{L} + \ldots \tag{16}$$

with $\dim q_{L,R} = N_\mathrm{f} \times n_{L,R}$ are Grassmann numbers, $\gamma_5 = (\mathbf{1}_\mathrm{R}, \mathbf{1}_\mathrm{L})$, and $n_\mathrm{L} + n_\mathrm{R} = V$. The $\ldots$ terms in (16) could be either singlets $(1,1)$, or non-singlets. The latters should vanish in the chiral limit as m^a with $a > 1$.

The finite volume partition function associated to (16) may be either cast in the Grassmann variables, or by bosonization through $\mathcal{A}^{ab} = q_\mathrm{L}^a q_\mathrm{R}^{b\,\dagger}$ which is $N_\mathrm{f} n_\mathrm{L} \times N_\mathrm{f} n_\mathrm{R}$, turned into an integral over bosonic matrices A in the form

$$\begin{aligned} Z[\theta, m] = \int \quad & d\mathcal{A}\, \mathrm{e}^{-V\Sigma \mathrm{tr}(\mathcal{A}^\dagger \mathcal{A}) + \ldots} \\ & \det \begin{pmatrix} im\mathrm{e}^{i\theta/N_\mathrm{f}} & \mathcal{A} \\ \mathcal{A}^\dagger & im\mathrm{e}^{-i\theta/N_\mathrm{f}} \end{pmatrix} . \end{aligned} \tag{17}$$

The determinant is $V \times V$ for $N_\mathrm{f} = 1$. From our preceding arguments, it does not matter what $\ldots$ is in the microscopic limit $mV < 1$. The finite volume partition function (17) is that of a chiral random matrix model. In QCD the quarks are in the complex representation, so A is a complex valued matrix. The chiral random matrix ensemble generated by the description (17) is ChGUE.

5.2. Without GOR

The minimal four-fermi model in 0-dimension that is commensurate with (6) is

$$\begin{aligned} \mathcal{L} = \quad & q^\dagger \; im\mathrm{e}^{i\gamma_5\theta/N_\mathrm{f}} \; q + REDA0.b.tex4V\Sigma^2 \Big[\; q_\mathrm{R}^\dagger q_\mathrm{L} q_\mathrm{R}^\dagger q_\mathrm{L} \\ & + REDA0.b.tex(B+C)V \left((q_\mathrm{L}^\dagger m^\dagger q_\mathrm{L})^2 + (q_\mathrm{R}^\dagger m q_\mathrm{R})^2 \right) \\ & + 2REDA0.b.tex(B-C)V (q_\mathrm{R}^\dagger q_\mathrm{R})(q_\mathrm{L}^\dagger m m^\dagger q_\mathrm{L}) \Big] \\ & + D\mathrm{Tr}(m^\dagger m) + \ldots \end{aligned} \tag{18}$$

Again, $\ldots$ are either singlets or non-singlets but then of higher order in m. The finite volume partition function can be bosonized using: $\mathcal{A} = q_\mathrm{L} q_\mathrm{R}^\dagger$,

$\mathcal{B}^R = q_{\rm R} q_{\rm R}^\dagger$ and $\mathcal{B}^L = q_{\rm L} q_{\rm L}^\dagger$, the result is a multi-random matrix model ($N_{\rm f} = 1$)

$$\begin{pmatrix} im{\rm e}^{i\theta} + m{\rm e}^{i\theta}\mathcal{B}^R & \mathcal{A} \\ \mathcal{A}^\dagger & im{\rm e}^{-i\theta} + m{\rm e}^{-i\theta}\mathcal{B}^L \end{pmatrix} \tag{19}$$

with width of the distribution given by

$$\begin{aligned} \left\langle \mathcal{B}^L_{ab}\mathcal{B}^L_{cd}\right\rangle &= \left\langle \mathcal{B}^R_{ab}\mathcal{B}^R_{cd}\right\rangle = REDA0.b.tex1\sqrt{V}\cdot REDA0.b.tex8(B+C)\Sigma^2\delta_{ad}\delta_{bc}, \\ \left\langle \mathcal{A}_{ab}\mathcal{A}^\dagger_{cd}\right\rangle &= REDA0.b.tex1V\cdot REDA0.b.tex1\gamma_{\rm EFF}\,\delta_{ad}\delta_{bc}\,, \end{aligned} \tag{20, 21}$$

where

$$REDA0.b.tex1\gamma_{\rm EFF} = REDA0.b.tex4\Sigma^2\left(1 + (B-C)REDA0.b.tex2m^2V\right). \tag{22}$$

The inverse bosonization of (18) using $q^\dagger_{R,L}q_{R,L}$ as bosonic variables can be shown to yield (6) as expected. In this case, the different scalings in V in the width (21) are important. The terms of order $({\rm Tr}U)^2$ follows only after an exact gaussian integration over $\mathcal{A}$ and $\mathcal{B}$ has been performed. We note that in the present formulation, (18) yields A in terms of B, C and Σ.

6. Microscopic spectral distribution

Since the microscopic sum rules follow from chiral random matrix models in the microscopic regime $mV < 1$, we can then use the powerful machinery of random matrix theory to make precise statements on the eigenvalue distribution and its correlation. Without loss of generality, we can just assume a gaussian weight in (17) and proceed. Throughout, we will discuss the GOR case. The alternative case is straightforward to implement.

6.1. Orthogonal polynomial method

Following Verbaarschot and Zahed [9], we may specialize to the symmetric case $n_{\rm L} = n_{\rm R} = V/2 = N$ (zero winding sector), and use the polar decomposition of the unitary matrix A, $A = U\Lambda V^\dagger$, where $\Lambda = {\rm diag}(\lambda_1, ..., \lambda_V)$ in $\boldsymbol{R}_+$, and U in ${\rm U}(V)$ and V in ${\rm U}(V)/{\rm U}(1)^V$. The division by ${\rm U}(1)^{\rm N}$ preserves the number of degrees of freedom. As a result, the angular and radial integration separates, the former inducing only an overall m-independent normalization. It will be ignored. With this in mind, we have

$$Z[N,m] = \int_0^\infty \prod_{i=1}^N d\lambda_i e^{V\Sigma\lambda_i^2} \prod_f^{N_{\rm f}} (\lambda_i^2 + m_f^2)\ \Delta[\lambda] \tag{23}$$

with the Vandermonde determinant

$$\Delta[\lambda] = \prod_{i<j} |\lambda_i|(\lambda_i^2 - \lambda_j^2)^2 \tag{24}$$

following from the Haar measure on SU(V) in the polar decomposition [25]. The first determinant in (23) stems from the integration over the Grassmannians.

In random matrix theory [22], the partition function (23) has a simple form in terms of the joint eigenvalue distribution

$$\nu(\lambda_1, ..., \lambda_V) = |\langle P_1 ... P_V | \lambda_1 ... \lambda_V \rangle|^2 \,, \tag{25}$$

where the P_i's form a set of ortho-normalized polynomials of degree i-1 with $1 \leq i \leq V$ (with the term of degree i normalized to 1), with the measure

$$\int_0^\infty d\lambda^2 \mathrm{e}^{-V\lambda^2} \prod_{f=1}^{N_\mathrm{f}} (\lambda^2 + m_f^2) P_i(\lambda) P_j(\lambda) = \mathbf{1}_{ij} \,. \tag{26}$$

The relation (25) follows simply from the properties of determinants (invariance under arbitrary linear combinations of either columns or rows). It is a Slater determinant with $P_1, \ldots P_V$ as the 'bra's and $\lambda_1, \ldots \lambda_V$ as the coordinate 'ket's. In particular,

$$\nu(\lambda) = \int d\lambda_2 ... d\lambda_N \; \nu(\lambda, \lambda_2, ... \lambda_V) = \sum_{i=1}^{V} |P_i(\lambda)|^2 \tag{27}$$

for the eigenvalue distribution at finite V and N_f. Eq. (25) summarizes all eigenvalue correlations.

In the microscopic regime $m < 1/V$. Consider the simplest case where $m = 0$, for which (26) is just the condition for the generalized Laguerre-Selin polynomials [9]. In the microscopic regime $V \to \infty$ with $V\lambda$ fixed, this distribution can be evaluated exactly in the form

$$\nu_s(x) = (\Sigma^2 x/2) \left(J_{N_\mathrm{f}}^2(\Sigma x) - J_{N_\mathrm{f}+1}(\Sigma x) J_{N_\mathrm{f}-1}(\Sigma x) \right) \tag{28}$$

in the sector with zero winding number. The dependence of $\nu_s(x)$ is shown in Fig. 5, for $N_\mathrm{f} = 0, 1, 2$. The larger N_f the wider the distribution at zero virtuality, following larger repulsion from the fermion determinant. In our case $\Sigma = 1$, but in general it is the scale associated to $\langle q^\dagger q \rangle$ in the chiral limit as is apparent from (4).

In a finite box, $\langle q^\dagger q \rangle$ gets renormalized by non-zero modes, and thereby develops a dependence on $1/L$ along with m (and of course Σ) as originally

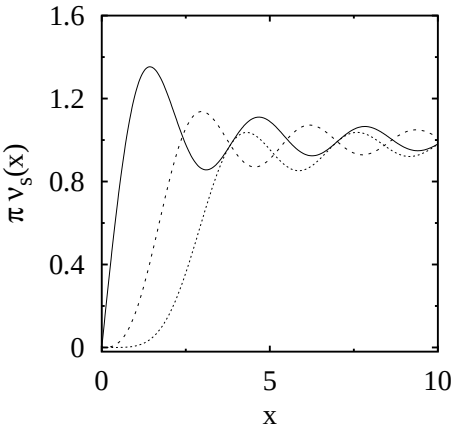

Fig. 5. Microscopic spectral distribution for ChGUE with $N_{\rm f} = 0$ (solid), $N_{\rm f} = 1$ (dashed), $N_{\rm f} = 2$ (dotted).

discussed by Hansen and Leutwyler [26]. We will refer to it as $\Sigma(m, L)$. Its dependence on the low energy parameters at the chiral point such as the pion decay constant, scattering length *etc.* along with $1/L$ and can be organized using a double book-keeping in ε and p.

The correlations between eigenvalues in the microscopic limit can be constructed using similar arguments. In particular, the connected correlator between two eigenvalues x and x' in the microscopic regime for $n = 0$ is [9]

$$\nu_s(x, x') = \Sigma^2 x x' \left(\frac{x J_{N_{\rm f}}(\Sigma x) J_{N_{\rm f}-1}(\Sigma x') - x' J_{N_{\rm f}}(\Sigma x') J_{N_{\rm f}-1}(\Sigma x)}{x^2 - x'^2} \right)^2 . \tag{29}$$

The connected two-point correlator (29) obeys the consistency condition

$$\int dx \; \nu_s(x, x') = 0 \tag{30}$$

which reflects on the conservation of the total number of eigenvalues. We will see below that the class of all n-point unconnected correlators may be resummed to give the microscopic eigenvalue distributions with $m \neq 0$ in the double scaling limit. Eq. (29) can be used to check the off-diagonal sum rules discussed by Leutwyler and Smilga [8]. The microscopic two-point correlator (29) may be used to address some issues related to the flavor admixture and spectral rigidity in the microscopic limit, as we now discuss.

As we have stressed above, the universality of (28) irrespective of the gaussian measure adopted is guaranteed by *(i)–(iii)* as discussed in Section 3.1, thanks to the modified power counting. These observations are of

course in agreement with those made by Nishigaki and Damgaard [27] in the context of polynomial weights. They are however more general, as they apply to a field theory. Although the present arguments apply to QCD in even-dimensions they can be easily modified to accommodate QCD in odd dimensions as discussed by Verbaarschot and Zahed [28]. This point is noteworthy as it implies that the issue of the instantons and a vacuum angle is not crucial for the present observations.

6.2. Flavor mixing

It was noted early on by Nowak, Verbaarschot and Zahed [23], that the eigenvalue correlator in the macroscopic limit reflects on important aspects of the QCD vacuum as a disordered medium. In particular, it was suggested using the instanton liquid model that the admixture of flavor (strangeness) is suppressed in the ground state (average of all n-states) if the instanton density is closer to the metallic regime. A measure of this suppression is given by the two-point correlator in the eigenvalue distribution, and could be directly related to the level variance in the macroscopic limit. Zweig's rule is supported by Wigner–Dyson statistics in the macroscopic limit.

In light of our present discussion, similar questions may be asked in the microscopic limit, for which it is easy to show that the Zweig's violating correlator investigated in [23], that is $\langle s^\dagger s u^\dagger u\rangle$ can be written in terms of (29) in the $n=0$ state with $y_i = m_i V$ as,

$$i^2\langle s^\dagger s u^\dagger u\rangle_0(y_u,y_s) = \int dx dx' \frac{y_u}{x^2+{y_u}^2}\frac{y_s}{x'^2+{y_s}^2}\nu_s(x,x'). \tag{31}$$

In particular,

$$\lim_{y\to 0}\frac{i^2\langle s^\dagger s u^\dagger u\rangle_0}{y_u y_s} = \frac{\Sigma^4}{16N_{\rm f}^2(N_{\rm f}+1)} \tag{32}$$

which is seen to break the cluster decomposition. The admixture of flavor in the microscopic limit in an n-state is universally given by the multipoint correlators in the microscopic limit.

6.3. Spectral rigidity

The microscopic spectral density $\nu_s(x,x')$ characterizes the level spacing distribution a quantum leap apart, not only at zero virtuality but also in the bulk of the spectrum. Indeed, it carries important information on the spectral statistics in the microscopic regime, such as the spacing distribution or the level variance. It also plays a major role at the interface of the theory

of disordered systems and the semiclassical theory of quantum chaos, as we will try to elaborate further on in the end.

To exemplify some of these points, let us consider in more detail the genealogy of Σ_2, the variance in the number of single particle levels within an energy interval $\Delta\lambda$ centered around λ_0, in the microscopic regime $\Delta x = V\Delta\lambda \gg 1$ but fixed as $V \to \infty$. This regime is characterized by constant mean density[2], $\nu_s(x) = \Sigma/\pi$, and in the decomposition of the full two point correlator, $\nu_s(x_1, x_2) = \nu_s(x_1)\nu_s(x_2)\delta(x_1 - x_2) - \nu_s(x_1)\nu_s(x_2)R(x_1, x_2)$, the cluster function $R(x_1, x_2)$ depends in the bulk only on the combination $s \equiv x_1 - x_2$ [29],

$$R(s) = \frac{\sin^2 \Sigma s}{(s\pi)^2} \tag{33}$$

for $s \neq 0$, the unitary ensemble and for any number of flavors. The level number variance, $\Sigma_2(N)$ is expressed through the cluster function R as

$$\Sigma_2(N) = \int_0^N dx_1\, dx_2\, R(s)\,. \tag{34}$$

Specifically, and for $\lambda_0 \neq 0$

$$\Sigma_2(N) = \frac{2}{\beta\pi^2} \log N \tag{35}$$

with $\beta = 2$. For the orthogonal and symplectic case $\beta = 1$ and 4 respectively. Both for the quenched and unquenched cases, the spectral rigidity is $2\ln N/(\beta\pi^2)$ as opposed to N for Poisson statistics. The decrease in the variance is an indication of a more rigid spectrum due to level repulsion [30].

6.4. Spacing distribution

The probability $P(s)$ to find two energy levels in the quark spectrum a distance s apart in the microscopic limit, that is $s = (\lambda_i - \lambda_j)V/\Delta$ fixed as $V \to \infty$, is also intimately related to the properties of the two-point correlator (29). For $s \ll 1$, that is as $\lambda_i \to \lambda_j$, we immediately see from the Vandermonde determinant (24) that $P(s) \sim s^\beta$ with $\beta = 2$. This is the usual level repulsion between two neighboring levels as predicted by Wigner [30]. It follows from the random lore for 2×2 matrices, since in this limit the rest of the eigenvalue spectrum decouples. Clearly it is independent of the number of flavors, except when one of the level is at zero virtuality. In this case, further repulsion is introduced by the fermion determinant and the winding number n in the massless case as is evident from Fig. 6.

[2] Actually this assumption is not really required, as unfolding procedures of spectra may be used [22].

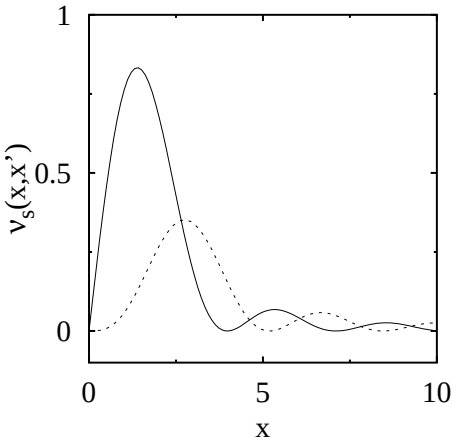

Fig. 6. Microscopic connected correlator for ChGUE $N_{\rm f} = 0$ (solid) and $N_{\rm f} = 1$ (dashed line) with an arbitrary normalization.

For $s \gg 1$ (still in the microscopic limit), the spacing distribution is solely governed by the asymptotics of the two-point correlator (29). For $R(s) \sim 1/\beta s^2$, the level distribution asymptotes $-\ln P(s) \sim \beta s^2$ as was shown by Dyson [29] using the the Coulomb gas treatment for (4) in the quenched case. In the unquenched case, the asymptotics of the two-point correlator is unaffected by the fermion determinant, resulting into the same level distribution. Indeed, for any $N_{\rm f}$, it is straightforward to see that the fermion determinant contributes to the potential term (one-body) not the interaction term (two-body). Since it is the latter that conditions the level spacing distribution, the self-quenching of this result is immediate. Hence, the whole level spacing distribution for (4) could be described by the standard Wigner surmise [30]

$$P(s) = As^{\beta} {\rm e}^{-B\beta s^2} \,, \tag{36}$$

where $\beta = 2$ and A, B are pure numbers. Which is drastically different from the Poisson distribution $P(s) = {\rm e}^{-s}$, for uncorrelated states.

6.5. Relevance to lattice

By now the present observations have been generalized to the case of finite winding number, as well as the two other Wigner ensembles: ChGOE and ChGSpE by Verbaarschot [31], and checked against lattice Dirac spectra by Schäfer, Weidenmüller and Wettig [32], and others [33]. In regard to the lattice measurements, we would like to point at few issues in regard to the strong coupling aspects of the simulation as well as the approach to the weak

coupling regime. Some of our remarks will also relate to certain aspects of the quenched approximation.

In strong coupling, the Kogut–Susskind action is characterized by an exact U(1)× U(1) symmetry. The analogue chiral random matrix model is ChGSpe [31]. So the strong coupling regime is characterized by universal microscopic spectral oscillations, even though Lorentz and full chiral symmetry are still absent. We also expect quantitative changes in the sum rules for quenched and unquenched simulations since the character of the coset and hence the number of Goldstone mode changes in this case [6].

In weak coupling, the Kogut–Susskind action is expected to undergo a transition to a phase with continuum Lorentz and full symmetry. A structural change from ChGSpe to ChGUE is therefore expected, for otherwise the true continuum would not have been reached. This point can be checked at the level of the microscopic sum rules, with due attention to scale translations, *e.g.* V, m (see below).

In symmetric boxes an accurate measurement of the finite volume chiral condensate in weak coupling can be reached by checking the microscopic sum rules, or simply monitoring the Bessel oscillations. This means an accurate assessment of the chiral condensate at order p^2, as well as the pion decay constant to the same order through possible finite volume effects.

In asymmetric boxes, the chiral condensate gets modified by temperature effects which can be assessed using a double expansion in ε and p (see below) at low temperature (small asymmetry). At high temperature, the chiral condensates disappears as the level spacing near zero becomes larger than $1/V$. For temperatures $T \sim T_c$, universality arguments may be used to argue for critical sum rules [34]. For $T > 3T_c$, the virtual spectrum is gapped by the lowest Matsubara mode $\lambda \sim \pi T$, except for thermodynamically irrelevant zero modes.

Finally, the relevance of the present concepts to lattice QCD in the strong coupling indicates that they are also applicable to lattice electronic systems with ferromagnetic or antiferromagnetic ground-state order. An example is the undopped Lanthanum–Copper–Oxide material for high temperature superconductors [35].

7. Double scaling regime

7.1. The formulae

In the transition regime $mV \sim 1$ the current quark masses affect the distribution of quark eigenvalues quantitatively for $N_{\rm f} \neq 0$, through the occurrence of the fermion determinant. Surprisingly enough, the non-local character of the latter supersedes the effects of local weights to upset the conventional universality arguments based on polynomial weights in the mi-

croscopic limit. This point was originally shown by Jurkiewicz, Nowak and Zahed [10] using the supersymmetric method for $N_{\rm f} = 1$ and zero winding number, and more recently by Damgaard and Nishigaki [11] and Wilke, Guhr and Wettig [12] using the orthogonal polynomial method with arbitrary $N_{\rm f}$ and winding number n [3].

The massive spectral density in the double scaling limit yields by definition the quark condensate in a fixed winding number configuration n, but with different m_s sea and m_v valence quark masses in general. Specifically,

$$i\langle q^\dagger q\rangle_n(\xi,y) = \int_0^\infty dx\, \frac{2\xi}{x^2+\xi^2}\nu_{s,n}(x,y) = \xi\Sigma_n^2(\xi,y) \tag{37}$$

with the rescaled valence quark mass $\xi = \Sigma m_v V$ and a finite sea quark mass $y = \Sigma m_s V$. We are using different notations for ξ, y to highlight their different origins. For $\xi = y$ the result is just the massive quark condensate in a winding number configuration n. The physical quark condensate with $\xi = y$ follows by suitably averaging over all windings n. For $N_{\rm f} = 1$ and $n = 0$ the massive spectral density is ($x = \Sigma V\lambda$)

$$\begin{aligned}\frac{1}{\Sigma^2}\nu_{s,0}(x,y) &= \frac{x}{2}\left[J_0^2(x) + J_1^2(x)\right]\\ &-\frac{J_0(x)}{I_0(y)}\frac{x}{x^2+y^2}\left[yJ_0(x)I_1(y) + xJ_1(x)I_0(y)\right]\end{aligned} \tag{38}$$

for $x > 0$. For $y = 0$ (38) reduces to (28) with $N_{\rm f} = 1$.

7.2. Sum rules

The microscopic spectral density (38) yields new microscopic sum rules with sea quark effects included. These sum rules are not a priori amenable to the finite volume partition function discussed above simply because (38) selects solely the sea quark mass effect, which is not a physical concept. Finite volume partition functions for QCD with different sea and valence quark masses can of course be simply constructed by using quark ghost fields [6]. Such discriminations are easily achievable on the lattice, and hence are of theoretical relevance. An example being the detailed valence quark study undertaken recently by Chandrasekharan and Christ [13], for a fixed sea quark mass contribution.

[3] Incidentally, this construction applies to any additive part one adds to the fermion determinant say T provided that it is suitably rescaled $T \to VT$ fixed, in the microscopic regime.

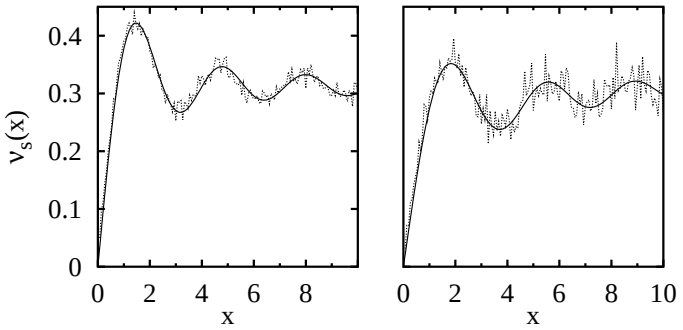

Fig. 7. Massive microscopical spectral density from an ensemble of 50000 $N = 50$ random matrices (dotted line) for $m_s = 1$ (left) and $m_s = 0.1$ (right), $N_{\rm f} = 1$, and the analytical formula (38) (solid line).

The derivative of (37) with respect to the valence quark mass generates a string of sum rules that are now sensitive to the effects of the sea quark mass y. Specifically, for $n = 0$, $N_{\rm f} = 1$, and fixed ξ, y

$$\frac{1}{V^2}\left\langle\left\langle {\sum_k}' \frac{2}{\lambda_k^2 + m_v^2}\right\rangle\right\rangle_0 = \Sigma_0^2(\xi, y)\,, \tag{39}$$

where the double averaging on the left-hand side involves $m^{|n|}\prod_k'(\lambda_k^2+m_s^2)$ as part of the measure, in contrast to the one used in (12) with $m_s = 0$. $\Sigma_0(\xi, y)$ depends on the rescaled valence and sea quark masses independently. Its analytical form is

$$\begin{aligned}\frac{\Sigma_0^2(\xi, y)}{\Sigma^2} &= I_0(\xi)K_0(\xi) + I_1(\xi)K_1(\xi) \\ &\quad + \frac{2K_0(\xi)}{y^2 - \xi^2}\left(\xi I_1(\xi) - \frac{yI_1(y)}{I_0(y)}I_0(\xi)\right)\,. \end{aligned}\tag{40}$$

For $y = 0$ it is in agreement with the result discussed by Verbaarschot [36]. In the limit of equal sea and valence quark masses the expression simplifies to

$$\frac{\Sigma_0^2(\xi, y = \xi)}{\Sigma^2} = \frac{I_1(\xi)}{\xi I_0(\xi)}\,. \tag{41}$$

In Fig. 8(a) we show the behavior of $\Sigma_0(\xi, y)/\Sigma$ for $y = 0$ (plus signs), $y = \xi$ (crosses), $y = 5\xi$ (triangles) and for fixed $m_s = 1$, that is $y = 1/N$ (boxes) from numerical simulation of 5000 $N = 50$ random matrices and the corresponding analytical form (40) (lines). For fixed and finite sea quark

mass Eq. (39) diverges as for small ξ as $-\log\xi$. In Fig. 8(b) we show the behaviour of the $n = 0$ condensate from (28) for the same set of masses, namely $y = 0$ (solid line), $y = \xi$ (dashed line), $y = 5\xi$ (dotted line) and fixed $m_s = 1$ (dashed-dotted line) .

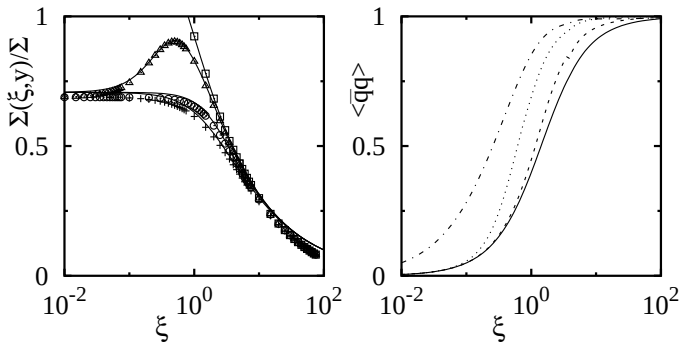

Fig. 8. (a) Sum rule (39) obtained numerically from an ensemble of 5000 $N = 50$ random matrices and the analytical result. (b) The quark condensate for various masses. See text.

For two massive sea quarks the result for the microscopic spectral density was worked out by Damgaard and Nishigaki [11], and Wilke, Guhr and Wettig [12] for arbitrary n. In this case, the analogue of (40) is

$$\begin{aligned}
&\frac{\Sigma_0^2(\xi,y_1,y_2)}{\Sigma^2} = I_0K_0 + I_1K_1 \\
&-\frac{y_1^2-y_2^2}{y_1I_1^aI_0^b-y_2I_0^aI_1^b}\frac{2}{y_1^4(y_2^2-\xi^2)+y_2^4(\xi^2-y_1^2)+\xi^4(y_1^2-y_2^2)} \\
&\times\Big\{y_1y_2I_1^aI_1^b\left[(y_1^2-y_2^2)I_0K_0+(y_2^2-\xi^2)I_0^aK_0^a+(\xi^2-y_1^2)I_0^bK_0^b\right] \\
&+(y_1I_1^aI_0^b+y_2I_1^bI_0^a)\left[\xi(y_1^2-y_2^2)I_0K_1+y_1(y_2^2-\xi^2)I_0^aK_1^a\right. \\
&\left.+y_2(\xi^2-y_1^2)I_0^bK_1^b\right] - I_0^aI_0^b \\
&\times\left[\xi^2(y_1^2-y_2^2)I_1K_1+y_1^2(y_2^2-\xi^2)I_1^aK_1^a+y_2^2(\xi^2-y_1^2)I_1^bK_1^b\right]\Big\}
\end{aligned} \tag{42}$$

with $I_i = I_i(\xi), I_i^a = I_i(y_1)$ and $I_i^b = I_i(y_2)$, respectively and similarly for K's. For one massive quark and $N_{\rm f} - 1$ massless quarks, the sum rule is given by

$$\frac{\Sigma_0^2(\xi,y)}{\Sigma^2} = I_{N_f}K_{N_f} + I_{N_f-1}K_{N_f+1} \tag{43}$$

$$-\frac{y^2}{N_{\rm f}(y^2-\xi^2)}\Big[I_{N_f-1}K_{N_f+1}-I_{N_f-1}(y)K_{N_f+1}(y)\Big]$$
$$+\frac{y^2 I_{N_f+1}(y)}{N_{\rm f}I_{N_f-1}(y)(y^2-\xi^2)}\Big[I_{N_f-1}K_{N_f-1}-I_{N_f-1}(y)K_{N_f-1}(y)\Big]\,.$$

For one massive quark and $N_{\rm f}-1$ massless quarks, the sum rule for the massive quark is $\Sigma^2(y,y)=\Sigma^2 I_{N_{\rm f}}/2yI_{N_{\rm f}-1}$ for $n=0$ as also noted by Damgaard [11]. We note that in this case $Z=Z_0$, which is the partition function in the $n=0$ sector. In particular, $i\langle q^\dagger q\rangle = i\langle q^\dagger q\rangle_0$. Additional sum rules involving diagonal and off-diagonal eigenvalue correlations are of course possible. The off-diagonal ones will involve the n-point correlation functions of eigenvalues with massive quarks.

Recently Chandrasekharan and Christ [13] have analyzed in details the behavior of the valence quark condensate for fixed sea quark mass $m_s a = 0.01$, for staggered $N_{\rm f}=2$ QCD, over several decades of the valence quark mass in an asymmetric lattice $V=4\times 16^3 a^4$. Their analysis was carried for various lattice coupling $\beta=6/g^2$ (varying lattice spacing a), around the chiral transition point $\beta_c=5.275$. Their underlying quark spectrum is clearly sensitive to temperature, and an analysis of this point using a macroscopic model distribution was discussed by Nowak, Papp and Zahed [37]. For small asymmetries, $\beta<\beta_c$, we may still assume that the conditions *(i)–(iii)* summarized at the end of Section 3.1 are still valid, in which case $i\langle q^\dagger q\rangle_0(\xi,y)$ may be amenable to a lattice comparison. For that, we need to identify $\Sigma_{\rm L}a^3$ for different β and the proper dimensionless combination $\xi_{\rm L}=m\Sigma_{\rm L}V$ on the lattice. For the former, we have: $\Sigma_{\rm L}a^3=0.2217$ ($\beta=5.245$), $\Sigma_{\rm L}a^3=0.1357$ ($\beta=5.265$) and $\Sigma_{\rm L}a^3=0.0543$ ($\beta=5.270$).

In the left part of Fig. 9 we show the lattice results for the normalized condensate versus the rescaled valence quark mass, $\xi_{\rm L}$. The line is the zero flavor result [36] in the $n=0$ topological sector seemingly in good agreement with the two flavor lattice data (symbols for different β's). In the right we show the two flavor result (42) for equal valence masses, $y=m_v\Sigma V$. The solid lines represent $N_{\rm f}=0,1,2$ massless flavors [36], respectivelly, the plus signes are for the lattice data with $\beta=5.245$ while the crosses for $\beta=5.270$. We conclude that the applied valence sea on the lattice is still to large making the system to be similar a quenched one ($N_{\rm f}=0$). Decreasing the valence sea by a factor of ten we start to see the deviation from the quenched result (boxes), and lowering the mass by a factor of hundred we recover the $N_{\rm f}=2$ zero mass limit (triangles).

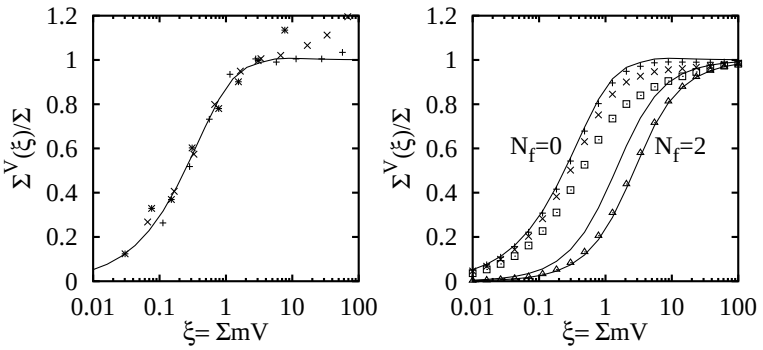

Fig. 9. Normalized condensate. See text.

For small valence quark mass $\xi < 0.1$ limit of Eq. (40), we find

$$\frac{\Sigma_0^2(\xi, y)}{\Sigma^2} = -\left(\log\frac{\xi}{2} + \boldsymbol{C}\right)\left(1 - \frac{2I_1(y)}{yI_0(y)}\right) + \frac{1}{2}\,. \tag{44}$$

In the large sea mass limit we recover the quenched limit, $-\log\xi/2 - \boldsymbol{C} + 1/2$ with a logarithmic divergence.

7.3. Universality

The result (38) is universal for the QCD spectrum as we now show. Following Smilga and Stern [38], we can rewrite the massive fermion determinant for a fixed background as ($n = 0$)

$$\begin{aligned} \Delta_m &= \prod_{\lambda_k > 0} (\lambda_k^2 + m^2)^{N_{\rm f}} \\ &= \Delta_0 \exp\left(N_{\rm f} \sum_{\lambda_k} \ln\left(1 + \frac{m^2}{\lambda_k^2}\right)\right)\,. \end{aligned} \tag{45}$$

Hence, the density of eigenvalues for finite m reads

$$\rho(\lambda, m) = \frac{1}{V}\left\langle \exp\left(N_{\rm f}\int_0^\infty d\lambda'\ \omega(\lambda', A)\ \ln\left(1 + \frac{m^2}{\lambda'^2}\right)\right)\omega(\lambda, A)\right\rangle_A\,, \tag{46}$$

where the averaging is over A including Δ_0, the fermion determinant with zero mass quarks, and $\omega(\lambda, A)$ is the unaveraged spectral operator

$$\omega(\lambda, A) = \sum_k \delta(\lambda - \lambda_k[A])\,. \tag{47}$$

In terms of the rescaled variables $x = V\lambda$ and $y = Vm$, the expression (46) reads

$$\nu_s(x,y) = \left\langle \exp\left(N_{\rm f} \int_0^\infty dx'\ \omega(x',A)\ \ln\left(1+\frac{y^2}{x'^2}\right)\right)\omega(x,A)\right\rangle_A \tag{48}$$

which involves all the moments of the microscopic spectral distribution. Specifically,

$$\nu_s(x,y) = \nu_s(x) + N_{\rm f}\int_0^\infty dx'\ \ln\left(1+\frac{y^2}{x'^2}\right)\langle\omega(x',A)\ \omega(x,A)\rangle_A + \dots \tag{49}$$

which is the weighted density-density correlator (second moment) in the microscopic limit. Each of the expectation value is carried in the n=0 state with massless quarks. All the moments are universal and given by random matrix theory. For $N_{\rm f} = 1$ the result for (48) is (38).

7.4. Range of validity

Since $mV \sim 1$ is the transition region in which the quark condensate (5) is no longer averaging to zero, the pionic zero modes in (3) are no longer dominant. What is the range of validity of (38) in QCD? The answer follows by noticing that (2) can be extended to one extra dimension, that is a Lagrangian in 1+4 dimensions. The support on the fifth direction is $[0,\beta]$ with periodic boundary condition for $U(x_5+\beta,x) = U(x_5,x)$. Here β plays the role of a 'temperature' and $-\ln Z/\beta$ for large β is just the ground state energy of the singlet Hamiltonian described by

$$\boldsymbol{H}_{1+4} = \frac{\vec{\boldsymbol{L}}^2}{2V} - \frac{mV}{2}{\rm Tr}(U+U^\dagger)\,, \tag{50}$$

where $\vec{\boldsymbol{L}}^2$ is the Laplace–Beltrami operator on the SU($N_{\rm f}$) manifold. Note that the present construction is analogous to the one discussed by Leutwyler [39] in $1+3$ dimensions.

For $mV = 0$ the spectrum is that of a spherical top with the irreducible representations of SU($N_{\rm f}$) as eigenfunctions. The spectrum is $1/V$ spaced with a mass gap. The ground state wavefunction is a constant on SU($N_{\rm f}$). The first excited state is $N_{\rm f}^2$ degenerate. For $mV \le 1$ the degeneracy is lifted. For $N_{\rm f} = 2$, the degeneracy is 4 with a triplet (pions) and a singlet (sigma) state. With increasing mV, the triplet states are pushed down and the singlet state up. The former merge into the physical pion mass as shown schematically in Fig. 10. We note that $m < 1/V$ puts the mass range into

the ergodic regime, and $1/V < m < 1/\sqrt{V}$ to the diffusive regime [14]. The transition to the macroscopic regime with a mass gap given by $\sqrt{m}$ (remember that $m_\pi^2 = 2m$ with our conventions) sets in for $mV \sim 10$.

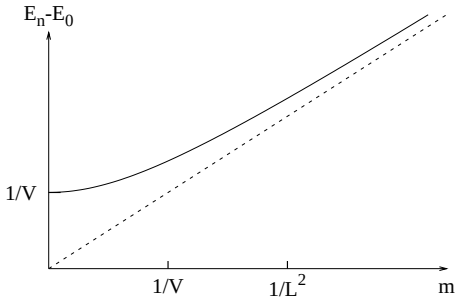

Fig. 10. Mass gap *versus* m from (50).

7.5. New results

Recently Damgaard [11] has suggested an interesting relation for $\nu_s(x,y)$ in terms of the finite volume partition function involving $1+2$ flavors with respective masses (y, ix, ix), using a property of the chiral random matrix measure. Generically, the microscopic spectral density reads [11]

$$\rho(\lambda) = C \cdot |\lambda| \prod_i (\lambda^2 + m_i^2) \frac{Z(m_1, \ldots, m_{N_\mathrm{f}}, i\lambda, i\lambda)}{Z(m_1, \ldots, m_{N_\mathrm{f}})}\,, \tag{51}$$

Schematically it means that

$$\langle \delta(z-\lambda) \rangle = \left\langle \prod (\lambda_i - z)^2 \right\rangle \cdot |\lambda| \prod_i (\lambda^2 + m_i^2)\,, \tag{52}$$

i.e. we may trade in a Dirac delta function for two *additional* flavours with imaginary masses. The origin of this formula in the random matrix model is very simple. One has just to insert the Dirac delta function into the expression of the RMM partition function written in terms of an integral over eigenvalues. Then the two flavours and the factors outside the expectation value just follow from contracting with the Vandermonde determinant. The term with the probability distribution $\mathrm{e}^{-NV(M)}$ does not contribute in the microscopic limit.

One would like to understand this formula from the point of view of QCD. The main difficulty is that in this regime of QCD, we are dealing only with the Goldstone boson degrees of freedom and all the explicit dependence on the spectrum of the Dirac operator seems to have been lost. In particular the low lying states are composite states in terms of the quark fields.

The main unsolved problem is to find an operator in the mesonic picture whose expectation value would correspond to the microscopic spectral density [40].

8. Macroscopic regime

In the macroscopic regime $mV > 1$, the constant modes in (3) cease to have a preferential role, and we are back to full QCD with (2), (6) (or even other unexplored power countings) as starting points in power counting.

However, there are a number of problems in QCD where power counting (in the sense exposed) breaks down. Examples are the strong CP problem, the U(1) problem, and phase transitions to cite afew. Since these problems involve in an intricate way the issues of large volumes, small quark masses, zero modes *etc.* it is useful to address in a framework where these quantities are simply separated in a way that allows for an analytical treatment. More importantly, the framework should be able to include some generic dynamical aspects of QCD in the form of few vacuum moments and symmetry.

The chiral random matrix models introduced above for studying the microscopic character of Dirac spectra, offer such an example. In many ways they can be regarded as a schematic description of the chiral physics at work in a cooled lattice QCD configuration within a finite Euclidean box V. Since these models allow for closed form results in terms of m, V, $N_{\rm f}$, *etc.*, they are very useful for addressing some subtle aspects of the thermodynamical limit in the presence of zero or near-zero modes whether in vacuum or matter.

8.1. Wide correlators

Chiral correlations in QCD involve usually eigenvalues which are separated by a macroscopic distance in the Dirac spectrum. They are defined for $V \to \infty$ and fixed $\lambda_i - \lambda_j$. Correlations over these distances will be discussed in this part of the lecture. For bounded spectra, Ambjørn, Jurkiewicz and Makeenko [41] have shown that the smoothened n-point correlation functions could be classified by the support of the spectral densities, independently of the specifics of the random ensemble and genera of the topological expansion. In QCD the Dirac spectrum is not bounded due to a strong ultraviolet tail $\rho(\lambda) \sim |\lambda|^3$. This tail, however, is not very important for infrared physics, except for multiplicative renormalization factors and anomalies. In a lattice formulation, this tail can be subtracted through a cooling procedure. The resulting spectrum is likely bounded, (except for possible tails which may be triggered by a partial loss of confinement), in which case the results discussed by Ambjørn, Jurkiewicz and Makeenko [41] for the hermitean case, and Janik, Nowak, Papp and Zahed [42] for the non-hermitean case may ap-

ply. An early account may be found in the analysis by Nowak, Verbaarschot and Zahed of the instanton liquid model [23].

8.2. U(1) problem

An important problem in QCD relates to the fact that the η' in nature is much more massive than the π, K, η system. It is believed that the discrepancy in mass is related to the fact that the U(1) current in QCD is anomalous. Indeed, using Ward identities it follows that (Minkowski space) [43]

$$i\chi_{\rm top} = -\frac{im}{N_{\rm f}^2}\langle\overline{q}q\rangle + \frac{m^2}{N_{\rm f}^2}\int d^4x\langle T^*\eta_0(x)\eta_0(0)\rangle\,, \tag{53}$$

where the topological susceptibility reads

$$\chi_{\rm top} = \int d^4x\langle T^*\Xi(x)\Xi(0)\rangle \tag{54}$$

and the topological density is $8\pi\Xi(x) = \alpha_s E^a\cdot B^a(x)$. The singlet current is $\eta_0(x) = \overline{q}i\gamma_5 q(x)$. For small m a gap in the singlet correlator requires that $\chi_{\rm top}\neq 0$. This is the presently accepted view for the resolution of the U(1) problem, although some difficulties may be noted [44].

The chiral random matrix models discussed in (17) offers a simple way to model some of the aspects of the present problem. Indeed, the matrix

$$\begin{pmatrix} ime^{i\theta} & A \\ A^\dagger & ime^{-i\theta}\end{pmatrix} \tag{55}$$

with entries $n_{\rm L}$ and $n_{\rm R}$ can be viewed as a schematic description of the topological zero modes in a finite volume V, with $\int\Xi = n_{\rm L} - n_{\rm R}$. Since γ_5 is just

$$\gamma_5 = \begin{pmatrix} \mathbf{1} & 0 \\ 0 & -\mathbf{1}\end{pmatrix} \tag{56}$$

it follows that the form of the anomaly in the present model is just $\mathrm{Tr}\,\gamma_5 = n_{\rm L} - n_{\rm R}$. The non-vanishing of (54) in QCD, will appear naturally in this model by summing over matrices of the type (55) as in (17) with varying sizes. The sizes will be gaussian distributed according to

$$\mathrm{e}^{-\frac{(n_{\rm L}-n_{\rm R})^2}{2V\chi_*}}\,. \tag{57}$$

Clearly $\langle(n_{\rm L}-n_{\rm R})^2\rangle = V\chi_*$ with the determinant set to 1 in (17) (quenched case).

This model has been discussed recently by Janik, Nowak, Papp and Zahed [45]. Their results are shown in Fig. 11, where the topological susceptibility (upper left), the pseudoscalar susceptibility (upper right) and the quark condensate (lower right) are studied versus m for different values of $N = n_{\rm L} + n_{\rm R} = V$. Clearly, the extrapolation to small values of m warrant larger and larger sizes N (volume V) for the result of Fig. 11 (upper right) to be meaningful. The solid curves are analytical results in the thermodynamical limit. The numerical results were obtained by sampling over matrices of different sizes using a Gaussian distribution for the matrix elements as in (17) and the distribution (57) for the size variations.

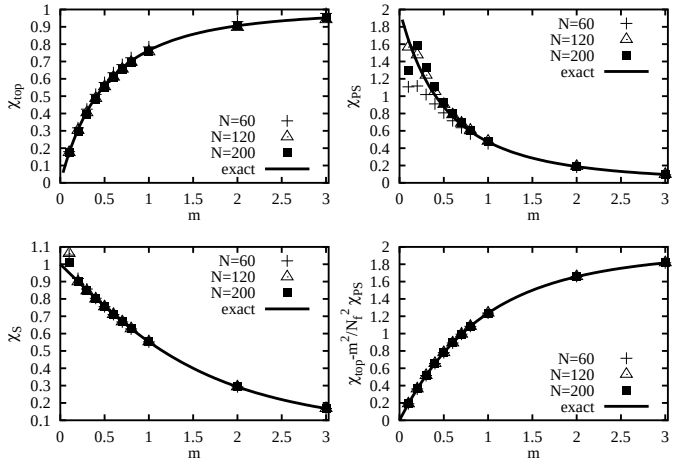

Fig. 11. Normalized topological (upper left), pseudoscalar (upper right), scalar (lower left) susceptibilities, and Ward identity (lower right) for $N_{\rm f} = 1$. The numerical simulations where carried for fixed $2N = n_+ + n_- = 60, 120, 200$ on an ensemble of 10^4, 5000 and 5000 matrices, respectively, and $\langle (n_+ - n_-)^2 \rangle = N\chi_\star = N$. The solid line is the analytical result [45].

8.3. CP problem

The non-vanishing of the topological susceptibility means that the vacuum partition function of QCD depends on the value of the vacuum angle θ. This point is also clear from our earlier arguments as the free energy $F(\theta, m, V) = -\ln Z[\theta, m, V]/V$ was θ dependent by construction. QCD with at small θ implies a free energy shift $F(\theta) - F(0) \sim \chi_{\rm top}\theta^2/2$, which violates T and P. Since strong interactions are known empirically to preserve T and P in the vacuum, this causes the strong CP problem.

A variety of scenarios have been put forward to resolve it ranging from axions to confinement [46]. This problem could have been in principle settled on the lattice if it were not for the breakdown of conventional Monte-Carlo algorithms at finite θ. Recently, Schierholz [47] has addressed this issue in the context of the CP^n model in two dimensions. His conclusions that the model exhibits a first order phase transition at finite θ were challenged by Plefka and Samuel [48].

Our present framework offers a testing ground for the present problem since both the issues of quenched, unquenched, finite size and current quark effects can be dealt with explicitly. As was shown by Janik, Nowak, Papp and Zahed [49] the model in many ways resemble the effective models discussed using effective Lagrangians in the saddle point approximation. The advantage, however, is that the present model allows for numerical simulations that test for the validity of such an assumption, the subtlety of the chiral and thermodynamical limit and the importance of the numerical accuracy.

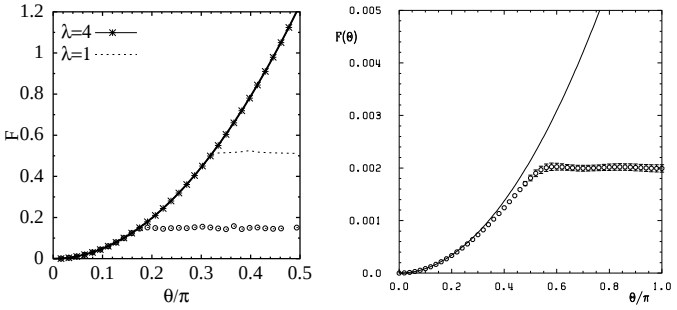

Fig. 12. ChRMM (quenched) partition function for N=250 (left). The normal precision calculation is shown by circles, the finite volume high precision by dashed line and the large volume high precision by solid line. Similar results are obtained for the unquenched pressure. CP^n model (right) [47].

9. Conclusions

We have reviewed some of the motivations in the introduction of chiral random matrix models to QCD problems, emphasizing some universal aspects in the microscopic limit as well as some generic aspects in the macroscopic limit. In particular, we have shown that by relaxing the GOR relation new microscopic sum rules and random matrix models may be set up in the context of QCD.

We have discussed the double scaling regime and we have presented relations for the chiral condensate in a fixed winding number sector, that are sensitive to the sea and valence quark masses independently.

In the macroscopic regime, we have suggested that ChRMM although not universal, exhibit generic aspects of the finite volume QCD problem that are useful for addressing currently open problems in QCD, with embarrassing similarities with bulk lattice simulations. ChRMM offer useful framework for understanding the interplay between the thermodynamical limit, the chiral limit and the precision of numerical algorithms.

Finally, we would like to conclude by pointing out that the chaotic aspect of the quark eigenvalues near zero virtuality as first revealed by random matrix theory from the finite volume partition function, may be established directly from QCD and general principles without recourse to power counting [14]. These arguments carry to lattice formulations as well as supersymmetric QCD.

These notes are based on the lectures and talks given recently by the authors at Kyoto (YKIS), Trento (ECT*), Cracow (Meson 98) and Zakopane (XXXVIII Course of Cracow School of Theoretical Physics). This work was supported in part by the US DOE grant DE-FG-88ER40388, by the Polish Government Project (KBN) grant 2P03B00814 and by the Hungarian grants FKFP-0126/1997 and OTKA-T022931.

REFERENCES

[1] S. Weinberg, *Physica* **96A**, 327 (1979).

[2] J. Gasser, H. Leutwyler, *Ann. Phys.* **158**, 142 (1984).

[3] H. Yamagishi, I. Zahed, *Ann. Phys.* **247**, 292 (1996).

[4] J. Gasser, H. Leutwyler, *Phys. Lett.* **B184**, 83 (1987); J. Gasser, H. Leutwyler, *Phys. Lett.* **B188**, 477 (1987); J. Gasser, H. Leutwyler, *Nucl. Phys.* **B307**, 763 (1988).

[5] P. Hasenfratz, H. Leutwyler, *Nucl. Phys.* **B343**, 241 (1990).

[6] T. Jolicoeur, A. Morel, *Nucl. Phys.* **B262**, 627 (1985).

[7] T. Banks, A. Casher, *Nucl. Phys.* **B169**, 103 (1980).

[8] H. Leutwyler, A. Smilga, *Phys. Rev.* **D46**, 5607 (1992).

[9] J.J.M. Verbaarschot, I. Zahed, *Phys. Rev. Lett.* **70**, 3852 (1993).

[10] J. Jurkiewicz, M.A. Nowak, I. Zahed, *Nucl. Phys.* **B478**, 605 (1996); Erratum, *Nucl. Phys.* **B513**, 759 (1998).

[11] P.H. Damgaard, S.M. Nishigaki, *Nucl. Phys.* **B518**, 495 (1998).

[12] T. Wilke, T. Guhr, T. Wettig, *Phys. Rev.* **D57**, 6486 (1998).

[13] S. Chandrasekharan, N. Christ, *Nucl. Phys. Proc. Suppl.* **47**, 527 (1996).

[14] R. Janik, M. Nowak, G. Papp, I. Zahed, *Phys. Rev. Lett.* **81**, 264 (1998).

[15] M. Gell-Mann, R.J. Oakes, B. Renner, *Phys. Rev.* **175**, 2195 (1968).

[16] J. Stern, H. Sazdjian, N.H. Fuchs, *Phys. Rev.* **D47**, 3814 (1993), and references therein.

[17] M. Baillargeon, P. Franzini, *Second DAPHNE Physics Handbook*, Eds. L. Mainani, G. Pancheri, P. Naver, Frascati 1995.

[18] E. Shuryak, J.J.M. Verbaarschot, *Nucl. Phys.* **A560**, 306 (1993).

[19] R. Alkofer, M.A. Nowak, J.J.M. Verbaarschot, I. Zahed, *Phys. Lett.* **B233**, 205 (1989).

[20] D.I. Diakonov, V.Y. Petrov, *Nucl. Phys.* B245, 259 (1984); D.I. Diakonov, V.Y. Petrov, *Nucl. Phys.* B272, 457 (1986).

[21] E. Shuryak, *Phys. Lett.* **B193**, 319 (1997).

[22] M.L. Mehta, *Random Matrices*, Academic Press, New York 1991.

[23] M.A. Nowak, J.J.M. Verbaarschot, I. Zahed, *Nucl. Phys.* **B325**, 581 (1989).

[24] Yu.A. Simonov, *Phys. Rev.* **D43**, 3531 (1991).

[25] L.K. Hua, *Harmonic Analysis, Translation of Mathematical Monographs*, Vol. 6. (1963).

[26] F.C. Hansen, *Nucl. Phys.* **B345**, 685 (1990).

[27] P.H. Damgaard, S.M. Nishigaki, *Phys. Rev.* **D57**, 5299 (1998).

[28] J.J.M. Verbaarschot, I. Zahed, *Phys. Rev. Lett.* **73**, 2288 (1994).

[29] F.J. Dyson, *Commun. Math. Phys.* **19**, 235 (1970); M.L. Mehta, *Commun. Math. Phys.* **20**, 245 (1971).

[30] E.P. Wigner, *Ann. Math. Phys.* **53**, 36 (1951); **62**, 548 (1955); **67**, 325 (1958).

[31] J.J.M. Verbaarschot, *Phys. Rev. Lett.* **72**, 2531 (1994); *Phys. Lett.* **B329**, 351 (1994); *Nucl. Phys.* **B427**, 434 (1994).

[32] T. Wettig, T. Guhr, A. Schäfer, H.A. Weidenmüller, in *QCD Phase Transitions*, Eds. H. Feldmeier *et al.*, Hirschegg 1997.

[33] M.E. Berbenni-Bitsch, S. Meyer, A. Schafer, J.J.M. Verbaarschot, T. Wettig, *Phys. Rev. Lett.* **80**, 1146 (1998).

[34] R. Janik, M. Nowak, G. Papp, I. Zahed, Critical scaling at zero virtuality in QCD, hep-ph-9804244.

[35] G. Shirane, Y. Endoh, R.J. Birgeneau, M.A. Kastener, Y. Hidaka, M. Oda, M. Suzuki, T. Murakami, *Phys. Rev. Lett.* **59**, 2340 (1987), and references therein.

[36] J.J.M. Verbaarschot, *Phys. Lett.* **B368**, 137 (1996).

[37] M.A. Nowak, G. Papp, I. Zahed, *Phys. Lett.* **B389**, 137 (1996).

[38] A. Smilga, J. Stern, On the spectral density of Euclidean Dirac operator, BUTP-93-19, IPNO-TH-93-37.

[39] H. Leutwyler, *Phys. Lett.* **B189**, 197 (1987); H. Leutwyler, *Nucl. Phys. (Proc. Suppl.)* **4**, 248 (1988).

[40] Very recently and after completing these notes, this problem was solved by P.H. Damgaard, J.C. Osborn, D. Toublan, J.J.M. Verbaarschot, hep-th/9811212.

[41] J. Ambjørn, J. Jurkiewicz, Yu.M. Makeenko, *Phys. Lett.* **B251**, 517 (1990).

[42] R.A. Janik, M.A. Nowak, G. Papp, I. Zahed, *Nucl. Phys.* **B501**, 603 (1997).

[43] R.J. Crewther, *Phys. Lett.* **B70**, 349 (1977).

[44] H. Yamagishi, I. Zahed, hep-th-9709125.

[45] R.A. Janik, M.A. Nowak, G. Papp, I. Zahed, *Nucl. Phys.* **B498**, 313 (1997).

[46] R. Peccei, H. Quinn, *Phys. Rev. Lett.* **38**, 1440 (1977); S. Weinberg, *Phys. Rev. Lett.* **40**, 223 (1978); F. Wilczek, *Phys. Rev. Lett.* **40**, 279 (1978); Y.S. Wu, A. Zee, *Nucl. Phys.* **258**, 157 (1985).

[47] G. Schierholz, *Nucl. Phys. Proc. Suppl.* **A37**, 203 (1994).

[48] J.C. Plefka, S. Samuel, *Phys. Rev.* **D56**, 44 (1997).

[49] R.A. Janik, M.A. Nowak, G. Papp, I. Zahed, to be published.